Environmental Engineering and Management Journal

January 2020, Vol. 19, No. 1, 143-156
http://www.eemj.icpm.tuiasi.ro/; http://www.eemj.eu

"Gheorghe Asachi" Technical University of Iasi, Romania

A BIOCHAR-BASED POINT-OF-USE WATER TREATMENT SYSTEM FOR THE REMOVAL OF FLUORIDE, CHROMIUM AND BRILLIANT BLUE DYE IN TERNARY SYSTEMS

Matthew Maya[1], Willis Gwenzi[1], Nhamo Chaukura[2,3]*

[1]Biosystems and Environmental Engineering Research Group, Department of Soil Science and Agricultural Engineering, University of Zimbabwe, P.O. Box MP167, Mt. Pleasant, Harare, Zimbabwe
[2]Materials Research (MatRes) Group, Chemistry Department, Bindura University of Science Education, P Bag 1020, Bindura, Zimbabwe
[3]Nanotechnology and Water Sustainability (NanoWS) Research Unit, College of Science, Engineering and Technology, University of South Africa, South Africa

Abstract

A large population worldwide, especially among poor communities, consumes polluted drinking water. Commonly used water treatment methods are ineffective for contaminants removal, while advanced treatment technologies are complicated and expensive. Although some column studies have been reported, most studies use batch experiments, and do not provide design parameters for up-scaling the treatment process. The objectives of this study were to: (1) synthesize and characterize biochars derived from *Brachystegia spiciformis* hardwood, (2) evaluate the adsorption performance in batch experiments, and (3) use column studies to determine the design parameters for a point-of-use (POU) water treatment device. Pristine biochar was the most effective compared to steam activated-biochar, and iron oxide activated biochar. Adsorption data showed that fluoride adsorption was described by the Freundlich model (r^2 = 0.939), while chromium (r^2 = 0.933), and BBD (r^2 = 0.55) data followed the Langmuir model. Column data were described by the Logit (r^2 = 0.99) and Thomas (r^2 = 0.99) models. Layered adsorbents showed more superior fluoride adsorption and required the lowest mass of adsorbent compared to mixed adsorbent columns. While further studies are required to fully optimize this treatment system, the results suggest that biochar based adsorbents can be effectively used in POU water treatment.

Keywords: adsorption, isotherms, remediation, water pollution

Received: March, 2019; Revised final: June, 2019; Accepted: September, 2019; Published in final edited form: January, 2020

1. Introduction

More than 660 million people worldwide rely on unimproved sources of drinking water with up to 200 million being exposed to excessive fluoride, chromium and brilliant blue dye concentrations in natural water sources (Arora and Tiwari, 2017; Gwenzi et al., 2017). Fluoride concentration above 1.5 mg/L in drinking water are influenced by geochemistry, coal burning, mineral matter and fluorapatite, and rocks (igneous, micas, fluorite, amphiboles, and apatite) such as exist in the Gokwe North Karoo aquifer, Zimbabwe (Mamuse and Watkins, 2016; Tobayiwa et al., 1991; Togarepi et al., 2012; WHO, 2011). Chromium concentrations above 5 µg/L are geogenic, whereas elevated brilliant blue dye dosages primarily result from textile industries and agricultural food processing (Sujitha and Ravindhranath, 2016; WHO, 2011). Studies have shown that household based drinking water treatment

* Author to whom all correspondence should be addressed: e-mail: nchaukura@gmail.com or nchaukura@buse.ac.zw; Phone: +263 782209671

methods such as boiling, chlorination, filtration (straining with a cloth/porous ceramic/sand), solar disinfection, sedimentation, and multi-barrier systems through addition of water tablets and filtration, are ineffective in inorganic contaminant removal (Ali, 2014; De Gisi et al., 2016; Tran et al., 2017; Wang et al., 2017; WHO, 2011; Zhang et al., 2015). Instead, sand filtration results in bio-film formation, and a high dose of chlorination potentially forms disinfection by-products, which are carcinogenic (Ali, 2014; Xue et al., 2017). Effective methods for inorganic contaminants removal such as reverse osmosis and ion exchange have complex treatment procedures, and high operational and maintenance costs (Gupta et al., 2009). Previous studies for the removal of pollutants such as Cr(IV) and fluoride have explored methods such as membrane capacitative deionization (Gaikwad and Balomajumder, 2018), electrocoagulation-electrofloatation (Aoudj et al., 2015), and adsorbents derived from agricultural waste (Hemavathy et al., 2019; Manikandan et al., 2018; Yaashikaa et al., 2019). Drinking water treatment by adsorption has several advantages including the use of locally available materials, high efficiency and selectivity, cost effectiveness, ease of operation and simplicity of design, high removal efficiency (>90%), while maintaining the taste and colour (Chaukura et al., 2017; De Gisi et al., 2016; Mohan et al., 2014). One such adsorbent, biochar, has been studied in the adsorption of a wide range of pollutants (e.g., Gwenzi et al., 2014; Oh et al., 2016; Wang et al., 2017).

Biochar is a porous carbonaceous material synthesized by the pyrolysis of biomass under low oxygen conditions. Consequently, it possesses a large surface area and good ion exchange capacity (Mohan et al., 2014; De Gisi et al., 2016). Previous studies showed that biochar can remove 90 % of heavy metals and other inorganics from aqueous solution (e.g., arsenic and fluoride, Chen et al., 2011; Zn and Ni., ; Dutta et al., 2012; Gwenzi et al., 2014; Mohan et al., 2012; Pb (II), Cr (VI) and As (V), Zhou et al., 2014). Either batch or continuous reactors are used in the preparation of biochar (Mohan et al., 2014). On the one hand, continuous reactors such as fixed and fluidized bed pyrolyzers are more complex and expensive to design and operate, and may require a reliable source of electricity (Duku et al., 2011; Gwenzi et al., 2015). On the other hand, batch reactors such as the metal and drum kiln, mound earth and pits, and the KonTiki flame curtain are relatively easy to design, handle and operate. Among batch reactors, the KonTiki reactor is the most efficient, where the feedstock is pyrolyzed in a smokeless fire (Schimidt and Taylor, 2014). The pyrolysis gases act as cover gas, creating air exclusion for producing high quality biochar in large quantities at low cost. This reactor also functions as a dryer and pyrolyzer, and its combustion is optimized by a rim shield (Schmidt and Taylor, 2014). Interestingly, there is little data on adsorption capacities of biochars from cookstoves such as KonTiki among other pyrolytic stoves.

Current literature on biochar is largely limited to biochar synthesis, reaction kinetics and isotherm behaviour of different biochar feedstocks, and the potential of biochar in contaminant removal from water. Where they exist, these studies mainly focus on single pollutants (e.g., Chaukura et al., 2017; Gwenzi et al., 2015; Mohan et al., 2014; Zhou et al., 2014). The majority of studies conducted on biochar technology were batch experiments and a few column experiments. Column studies have an advantage over batch experiments as they involve the determination of the total volume of influent and effluent, flow rate, depth of adsorption zone and percentage of total column saturated at breakthrough (Ali, 2014; Kumar and Acharya, 2012; Ndé-tchoupé et al., 2015). These parameters are essential inputs into the design of a functional prototype and the actual water treatment system.

In this study, a point-of-use (POU) water treatment system that uses biochar is designed for poor communities in developing countries and accounts for the following: (1) lack of money and small sparsely distributed populations, (2) lack of technical skills and knowledge to operate existing technologies, (3) lack of electricity to operate some existing affordable solutions such as electro-coagulation and reverse osmosis, and (4) supports the United Nations sustainable goal No. 6 of 'ensuring availability and sustainable management of clean water for all' (UN, 2015). In addition, this study capitalized on the unexploited opportunity of converting domestic fuel wastes (wood residues) from cooking and heating into biochar and its subsequent use for water treatment. The hypotheses tested were: (1) iron oxide activated biochar have significantly higher adsorption capacity than steam activated and pristine biochar adsorbents and sand (control) in batch experiments, and (2) layered biochar adsorbents have significantly high contaminant adsorption capacity than biochar and sand mixed in a column filter bed and sand filter (control) in column experiments. The specific objectives were: (1) to synthesize biochar based adsorbents derived from *Brachystegia spiciformis* hardwood using a KonTiki pyrolysis reactor, (2) to evaluate the adsorption capacities of the adsorbents through batch experiments, and (3) to determine the design parameters for a point-of-use prototype using data (hydraulic retention time, bed volume and flow velocities) from column experiments.

2. Material and methods

The study involved a combination of water sampling fieldwork and laboratory experimentation. This included: (1) sampling of fluoride contaminated water from Gokwe in western Zimbabwe (17.85473° S and 28.649 ° E), (2) synthesis and activation of wood biochar adsorbents; (3) evaluation of adsorbents through batch experiments; and (4) determination of point-of-use prototype design parameters using column experiments (Fig. 1).

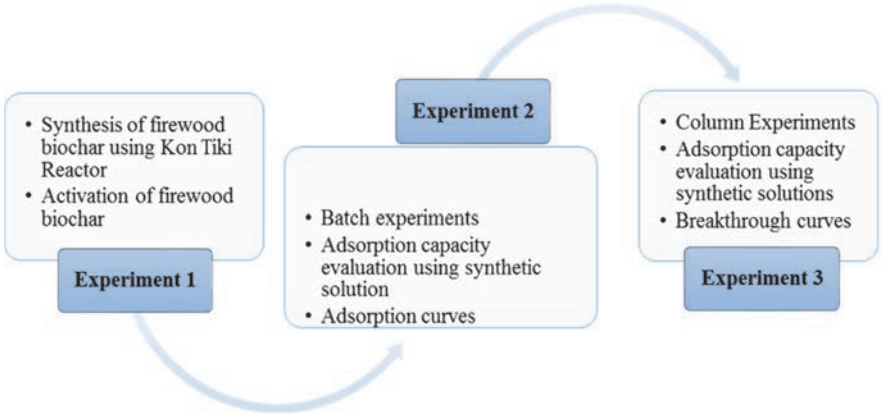

Fig. 1. Methodology process flow

2.1. Sampling

Water samples for fluoride analysis, and wood for biochar synthesis were collected from hot springs in Gokwe North, western Zimbabwe. The study site is dominated by drier miombo woodland, with Brachystegia spiciformis and Baikiaea plurijuga species (Vermeulen et al., 1996). The reason Brachystegia spiciformis was chosen is because of its availability in the local community, making the defluoridation technology accessible to local communities. The area lies in a semi-arid region where water supplies are limited and households rely on groundwater, which is saline and contains excessive fluoride (> 1.5 mg/L) (Mamuse and Watkins, 2016).

2.2. Preparation and characterization of adsorbents

The KonTiki flame curtain reactor was operated following procedures described by Schmidt and Taylor (2014). Briefly, Brachystegia spiciformis wood of size < 50 cm length, and < 10 mm diameter was used to facilitate the initial combustion. An open stacked square chimney of dry wood was built in the middle up to about three-quarters of the kiln height and the chimney was ignited from the top. The first regular layer of biomass was added when the biomass layering was coated with white ash. This was meant to maintain a potent flame front above the pyrolyzing material to consume down-convecting oxygen while combusting smoke. The process of adding biomass and observation of white coating was repeated for all the subsequent layers until quenching. A tap at the end of the reactor was connected to a water source 20 min before the pyrolysis of the last biomass layer.

Three biochar adsorbents were thus prepared, namely: (1) biochar activated by iron oxides prepared by spraying red soil and water mixture (red clay soil containing iron oxides mixed with water in 1:1 ratio) before quenching (Schmidt and Taylor, 2014) (Fe_2O_3-BC); (2) pristine biochar by quenching from the top of the reactor (BC); and (3) steam activated biochar by quenching from the bottom (SBC) (Schimidt and Taylor, 2014). The biochar was dried in a fiber glass drier at 30 °C for 48 h. Dried biochar was milled, passed through 2 mm and 1 mm sieves and washed with distilled water before oven-drying at 102 °C for 24 h. The biochar samples were further oven-dried for 24 h at 110 °C for the examination of surface morphology using scanning electron microscope-energy dispersive spectrometry (SEM-EDS) (Jeol JSM-IT300, USA) (Mishra et al., 2017), and surface functional groups using ATR-FTIR (Thermoscientific, Nicolet IS5). The surface morphology of adsorbents after adsorption was similarly evaluated.

2.3. Batch adsorption experiments

To investigate the adsorption capacities of the adsorbents, batch experiments were conducted using (1) Fe_2O_3-BC; (2) SBC; (3) BC, and (4) sand (control). Using three different stock solutions of 2000 mg/L NaF, $CrCl_3 \cdot 6H_2O$, and brilliant blue dye (BBD), ternary solutions of concentrations: (1) 15 F^-, 1.5 Cr, and 5 mg/L of BBD; (2) 10 F^-, 1.0 Cr, and 4 mg/L BBD; (3) 5 F^-, 0.5 Cr, and 3 mg/L BBD; (4) 3 F^-, 0.1 Cr, and 2 mg/L BBD; and (5) 1.5 F^-, 0.05 Cr, and 1 mg/L BBD, were prepared based on the permiscible drinking water guideline values and reported concentrations of inorganic and organic contaminants in natural drinking water sources (WHO, 2011). These concentrations were used in batch and column experiments to simulate the contaminated drinking water quality that can be found in the natural environment. The choice of pollutants was based on their toxicity and availability in the area of interest (Gaikwad and Balomajumder, 2018). Also included was brilliant blue dye to prove the concept that the synthesized materials can also remove related organics, which are possibly present in the drinking water.

Each adsorbent (2 g) was transferred into a 200-mL conical flask, and 100 mL of the ternary solutions added to achieve a solid-liquid ratio of 1:50 (Zhou et al., 2014). The mixture was shaken at 120 rpm on a mechanical shaker for 120 min at room temperature. The pH was maintained within a range of 5.1-6.0 by adding total ionic strength adjustment buffer solution. The mixture was then filtered through a Whatman No. 540 filter paper, and the filtrate was analyzed for F^-, Cr and BBD. A fluoride ion selective electrode (ISE

Eutech Instruments, model 9609BNWP) connected to an Ion 700 pH/mV/Ion/°C/°F Bench Meter was used to measure F^- concentrations, an atomic absorption spectrometer (AA spectra 50 Varian) was used for assaying Cr, and a UV-Vis spectrometer (Buck Scientific, 100 VIS) was used for measuring BBD concentrations. From these data, the adsorption capacity (Eq. 1) and percentage removal of contaminant (Eq. 2) were determined:

$$Q_t = \left(\frac{C_0 - C_t}{m}\right)V \quad (1)$$

$$\%removal = \left(\frac{C_0 - C_f}{C_0}\right)\times 100 \quad (2)$$

where Q_t (mg/g) is the amount of adsorbate per mass unit of adsorbent at time t; C_o and C_t (mg/L) are the initial concentration and concentration at time t of adsorbate; C_f is the final concentration; V is the volume of the solution (L), and m is the mass of adsorbent (g).

Based on the adsorption data, the adsorbent with highest F^-, Cr and brilliant blue adsorption was selected for detailed evaluation using column experiments. The adsorption data were fitted onto Langmuir (Eq. 3) and Freundlich (Eq. 4) isotherm models to describe the adsorption process:

$$\frac{q_e}{q_m} = \frac{bC_e}{1 + bC_e} \quad (3)$$

where q_e (mg/g) is the amount of adsorbate per mass unit of adsorbent at equilibrium; C_e (mg/L) is the liquid phase concentration of the adsorbate at equilibrium; q_m (mg/g) is the maximum adsorption capacity; b (L/mg) is the Langmuir constant related to the energy of adsorption.

$$\log q_e = \log K_F + \frac{1}{n}\log C_e \quad (4)$$

where K_F is the Freundlich isotherm constant (mg/g) $(m/g)^{-1/n}$); and $1/n$ is the Freundlich intensity parameter.

2.4. Column adsorption experiments

Column adsorption experiments were conducted as described by Kumar and Acharya (2012), Ndé-Tchoupé et al. (2015), and Okewale et al. (2015). The best performing adsorbent from batch adsorption evaluation was used in this experiment configured either in layers or mixed with sand as two treatments compared to sand as the control. Hence a total of three treatments were investigated: (1) BC layered in the filter bed; (2) BC and sand mixed in the filter bed as the adsorbent and (3) and slow sand filter as the control (Fig. 2).

Gravity-fed glass columns of 3 cm diameter and 24.2 cm length and a reactive zone of depth 10 cm were used. The filter bed was characterized by two sand layers with a thickness of 1.5 cm for physical bio-filtration and an adsorbent layer thickness of 7 cm. The pristine biochar adsorbent and sand sieved through a 1 mm sieve were packed in glass columns at 0.9 and 1.67 g/cm^3 packing density for biochar and sand, respectively. The columns were then soaked in deionized water at half the depth of column length for 24 h after packing, and the porosity (P) (Eq. 5) and pore volume (P_V) (Eq. 6) were determined (Ali, 2014; Mon et al., 2006):

$$P = 1 - \left(\frac{D_B}{D_S}\right) \quad (5)$$

where D_B is the bulk density (g/mL), and D_S the particle density (g/mL).

$$P_V = porosity \times p_v \quad (6)$$

where p_v is the packing volume of the column (mL).

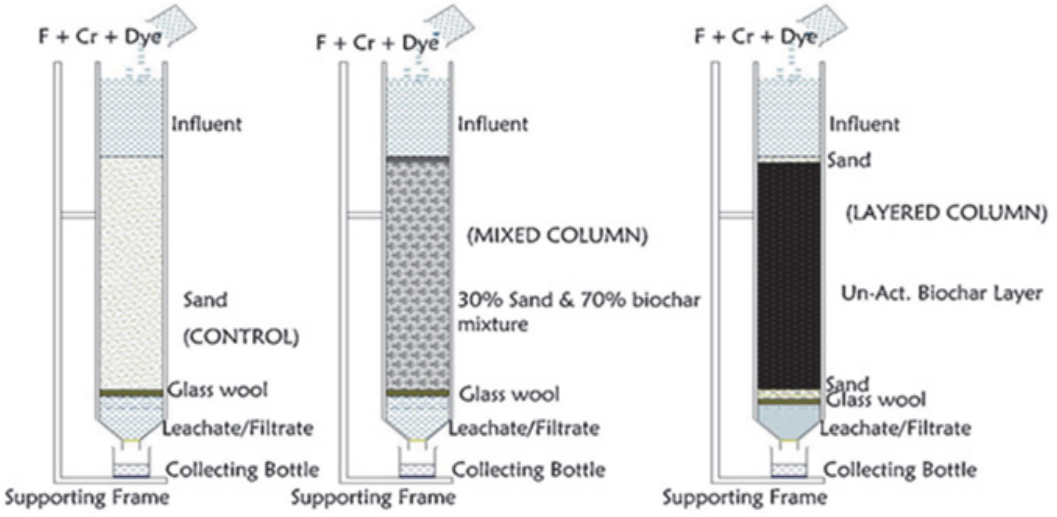

Fig. 2. Schematic column experiment set-up

A constant flow rate at the column feed head was 1.5 mL/mim throughout the experiments. The effluent concentrations were measured until they equaled the influent concentration, i.e. up to exhaustion point. Breakthrough curves were obtained by plotting the ratio of effluent concentration to influent concentration (C_e/C_o) as a function of pore volume at a given bed depth (Eq. 7 and Eq. 8) (Ali, 2014; Kumar and Acharya, 2012; Mon et al., 2006; Zhang et al., 2015):

$$B_p = (0.05 - 0.1) = \frac{C_e}{C_0} \quad (7)$$

$$E_p = (0.8 - 1) = \frac{C_e}{C_0} \quad (8)$$

where B_p is the breakthrough point, and E_p is the exhaustion point.

From column experiments, point-of-use prototype design parameters determined include: (1) media volume; (2) minimum filtration rate; (3) maximum filtration rate; (4) optimum bed depth and (5) mass of adsorbent in a predetermined volume of the reactive zone (V_{rz}). The volume of the reactive zone was calculated from Eq. 9 as (Ndé-tchoupé et al., 2015):

$$V_{rz} = \pi \times \left(\frac{D^2}{4}\right) H \quad (9)$$

where D is the diameter, and H the height of the column.

Each synthetic solution prepared in preliminary experiments was separately gravity fed through the filter bed, and the leachate was assayed for Cr, BBD and F^-. Column experiment data were fitted onto Thomas (Eq. 10) and Logit (Eq. 11) models to evaluate the characteristic design parameters of the fixed bed column:

$$\frac{C_t}{C_0} = \frac{1}{1 + \exp\left(\frac{K_{Th} q_e x}{Q} - K_{Th} C_0 t\right)} \quad (10)$$

where: K_{Th} is the rate constant of Thomas model kinetic coefficient (mL $min^{-1}mg^{-1}$); q_e is the equilibrium uptake per g of adsorbent (mg/g); and x is the total dry weight of adsorbent in column (g).

$$\ln \frac{C/C_0}{1 - C/C_0} = \frac{-KN_0X}{V + KC_0t} \quad (11)$$

where C is the concentration at any time t; C_o is the initial concentration (mg/L); V is the approach velocity (cm/L); X is the bed depth; K is the adsorption rate constant (L/mg.h); and N_o is the adsorption capacity coefficient (mg/L).

2.5. Statistical analysis of data

Unstacked one way ANOVA analysis was conducted for the determination of significance differences between Fe_2O_3-biochar, SBC and BC adsorbents and the sand control with F^-, Cr and BBD as response variables through Turkey's method of comparison in batch experiments. Batch adsorption data were fitted onto Langmuir and Freundlich isotherm models and the goodness of fit was evaluated using the coefficient analysis to determine r^2 (Grassi et al., 2012; Zhou et al., 2014). For column data, unstacked one way ANOVA analysis was performed to determine the significance differences between layered biochar, sand and biochar mixed and the control sand with F, Cr, and BBD as response variables. Column adsorption data were fitted onto Thomas and Logit models to evaluate the adsorption mechanism dynamics and the degree of fit was based on r^2. All descriptive statistical analyses were performed using the Minitab 16 software at probability level $p = 0.05$.

3. Results and discussion

3.1. Morphology, elemental composition, and surface functional groups of adsorbents

Scanning electron microscopy (SEM) images of the adsorbents before adsorption show porous surface and ridges connecting one clumped section to the other, as well as voids between the ridges for the Fe_2O_3-BC (Fig. 3a), a porous surface that is completely spaced within the adsorbent structure, absence of straws or rods for connecting the porous surfaces and more white sections for the SBC (Fig. 3b), single heaped structure and spaced constituents of the adsorbent structure for pristine biochar (Fig. 3c), and loosely packed and heaped points within the sand adsorbent (Fig. 3d).

The major difference in structural appearance of the SEM images before and after adsorption was evident by the ridged and clumped structures of deposited material, hence the adsorption of F^-, Cr, and BBD occurred within the adsorbents inner pore spaces and extended to the outer surface (Fig. 4).

Energy dispersive X-ray spectroscopy (EDS) data show that Fe_2O_3-BC contain O, Ca, and high Fe content, SBC has the highest O content, BC has the highest carbon and oxygen content, and sand contains the highest Si content (Table 1). As expected, the Cr content after adsorption increased for all the adsorbents, indicating retention of the metal. While the presence of high Fe content relative to C, Mg, O and P in Fe_2O_3-BC showed that iron activation was successful, steam activation was demonstrated by high O content compared to Ca, P, K and Mg. Pristine biochar only had C and O. Carbon in biochar is derived from the *Brachystegia spiciformis* biomass, while the oxygen is from the quenching water. Typically, sand had high Si, Al, Ca and Mg content.

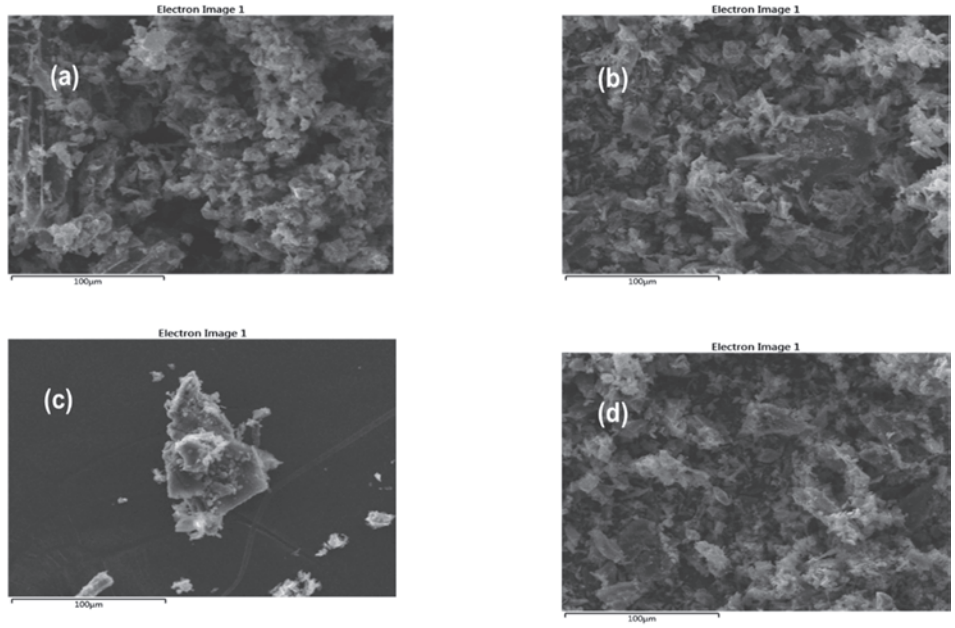

Fig. 3. SEM images for adsorbents before adsorption: (a) Fe_2O_3-BC, (b) SBC, (c) BC, and (d) sand

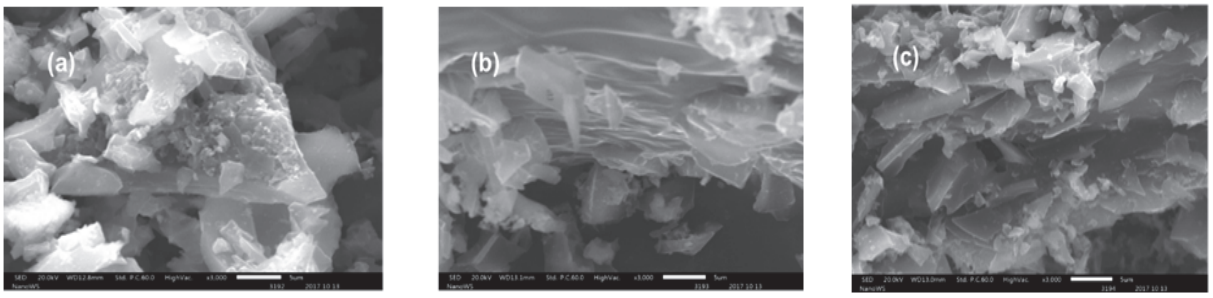

Fig. 4. SEM images for adsorbents after batch adsorption experiments: (a) BC, (b) SBC, and (c) Fe_2O_3-BC

Table 1. Elemental composition of the adsorbents before and after adsorption

	Content other than C (%)								
	O	Ca	Fe	K	Si	P	Al	Mg	Cr
Fe_2O_3-BC	47.0(45.1)*	25.0(24.1)	7.6(7.0)	5.9(5.2)	4.4(4.0)	4.1(3.8)	3.5(3.3)	2.5(2.3)	-(5.2)
SBC	59.2(54.2)	28.1(26.5)	-	4.9(4.4)	-	4.5(4.2)	-	3.3(3.0)	-(7.7)
BC	100(98.1)	-	-	-	-	-	-	-	-(1.1)
Sand	58.3(54.2)	27.0(25.3)	5.3(4.9)	-	4.2(3.8)	-	3.3(3.1)	1.9(1.4)	-(7.3)

**quantity in parentheses is the content after adsorption. A dash means the metal was not detected*

The presence of a cloudy appearance of deposited material in form of ridges, clumps and heaped surface on the SEM images of biochar adsorbents showed that F^-, Cr, BBD were adsorbed both inside and on the outer surface of the adsorbents. This is influence by the adsorption process that occurs at liquid-solid interface due to van der Waals forces or via chemical bonding resulting in the removal of F^-, Cr and BBD from synthetic solution and their subsequent accumulation on the solid surface (Ali, 2014; De Gisi et al., 2016; Okewale et al., 2015). Similar results were reported in previous studies (e.g., Kong et al., 2017; Mishra et al., 2017; Shang et al., 2016).

FTIR spectra show subtle dissimilarities between the adsorbents (Fig. 5). There is a significant peak for SBC around 3340 cm^{-1}, due to the OH groups introduced by steam activation. The peak is attributed to an inter-molecularly bonded O-H stretch, and is characteristic for alcohols, carboxylic, and phenolic moieties existent in cellulosic materials (Chaukura et al., 2017). The peak for BC around 1600 cm^{-1} is indicative of a C=C-C stretch, which is typical of an aromatic ring. The peak at 940 cm^{-1} is attributed to a =C-H bend. Barring the OH group, BC had no other oxygen-carrying groups, perhaps because the material was highly carbonized. Fluoride and Cr(IV) species being anionic are likely to have electrostatic interactions with the oxygen-carrying moieties and also with the electron dense multiple bonds. This is likely to result in repulsion and a decreased uptake of the pollutants. However, dative bonds between Cr and O should facilitate adsorption. Other mechanisms

could include π-π interactions between the aromatic groups on the adsorbent surface and the hexagonal structures of the adsorbents (Tong et al., 2019).

3.2. Batch experiments

The concentration of F^- in the water was in the range 9.93-14.68 mg/L, a range way above the WHO limit of 1.5 mg/L (WHO 2011). Previous studies showed that the water sampled from Gokwe had the following properties: 7.0<pH<8.3, 590<TDS<3210 mg/L, 1.2<EC<6.4 mS.cm^{-1}, 0.8<Mg<3.8 mg/L, 0.5<Ca<15.9, 14.1<Cl^-<607.7 mg/L, 2.4<SO_4^{2-}<1199.6 mg/L, and 4.4<F^-<11 mg/L (Mamuse and Watkins, 2016). The quality of water is expected to influence the removal of F^- and Cr(IV). For instance, adsorption is a pH-dependent process, and will thus be affected by the presence of protons in solution (Hemavathy et al., 2019; Yaashikaa et al., 2019).

3.2.1. Fluoride removal

Pristine biochar had the overall best defluoridation as F^- concentration increased from 0.5 to 15 mg/L compared to SBC and Fe_2O_3-BC (Fig. 6a). SBC is effective at low concentrations (0.5 to 5ppm), but this might not effectively address the problem of high F^- (15 mg/L) in Gokwe. Fe_2O_3-BC has a fairly constant adsorption capacity as concentration increases from 0 to 15 mg/L compared to BC but with significantly lower mean adsorption capacity in the range 10-15 mg/L. There was no significant difference between Fe_2O_3-BC, SBC, BC, and sand (p = 0.971) (Fig. 6a). Fe_2O_3-BC had the lowest defluoridation, and sand had the overall lowest among the experimental treatments.

3.2.2. Chromium removal

Pristine biochar had the highest Cr removal from concentration of 0.05 to 3 mg/L compared to SBC and Fe_2O_3-BC (Fig. 6b). The removal capacities for all adsorbents increased with an increase in initial concentration. Adsorption capacities of the adsorbents were similar from 0.05 to 1.5 mg/L, and started to differ from 1.5 to 3 mg/L. SBC had the lowest adsorption capacity, and sand had the overall lowest Cr removal. There was no significant difference between Fe_2O_3-BC, SBC, BC, and sand (p = 0.314) (Fig. 6b).

3.2.3. Brilliant blue dye removal

Pristine biochar had the overall highest BBD removal from 1 to 5 mg/L as compared to SBC and Fe_2O_3-BC (Fig. 6c). Steam-activated biochar had the highest removal capacity at low concentration (1-2.5 mg/L). As initial concentration increased from 2.5 to 4 mg/L, the adsorption capacity of SBC was lowest compared to other biochars. Fe_2O_3-BC had the lowest BBD adsorption capacity from 1 to 2 mg/L, then increased rapidly as the concentration increased from 2 to 5 mg/L as shown by steep gradient. Sand had the overall lowest adsorption capacity as shown by a decrease in equilibrium concentration with increasing BBD initial concentration. While there was no significant difference between Fe_2O_3-BC, SBC, and BC (p = 0.993), there was significant difference between Fe_2O_3-BC, SBC, BC against sand (p = 0) (Fig. 6c). The differences between Fe_2O_3-BC, SBC, and BC adsorption capacities were attributed to the different methods of quenching at the end of the synthesis stage (Schmidt and Taylor, 2014). Activating biochar with iron water solution has been reported to reduce pore spaces and the uptake of F^- and BBD, and increase the adsorption of Cr (Okewale et al., 2015). Bottom quenching for producing SBC is expected to be less effective than quenching from the top because downward flow results in increased ash content in biochar resulting in pore blockage and a decrease in adsorption capacity (Okewale et al., 2015).

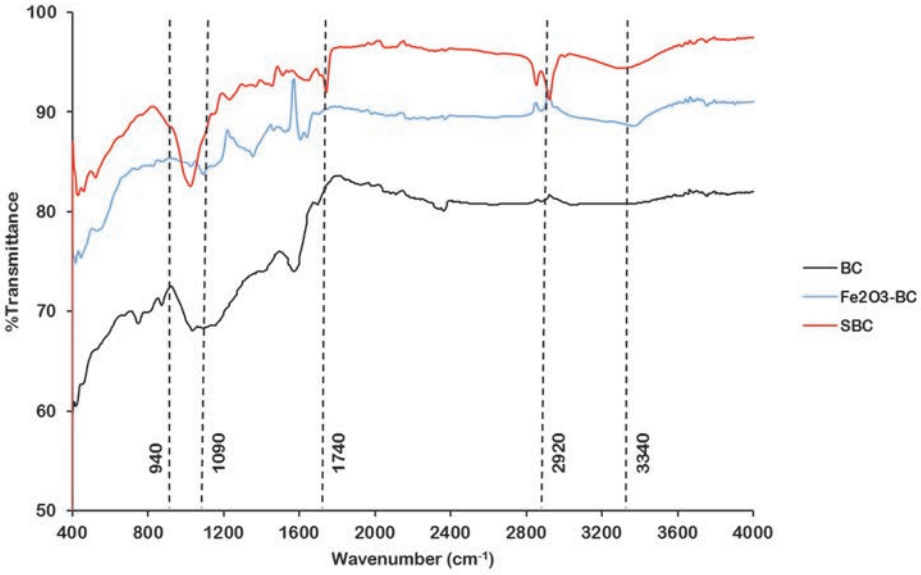

Fig. 5. FTIR spectra for BC Fe_2O_3-BC, and SBC

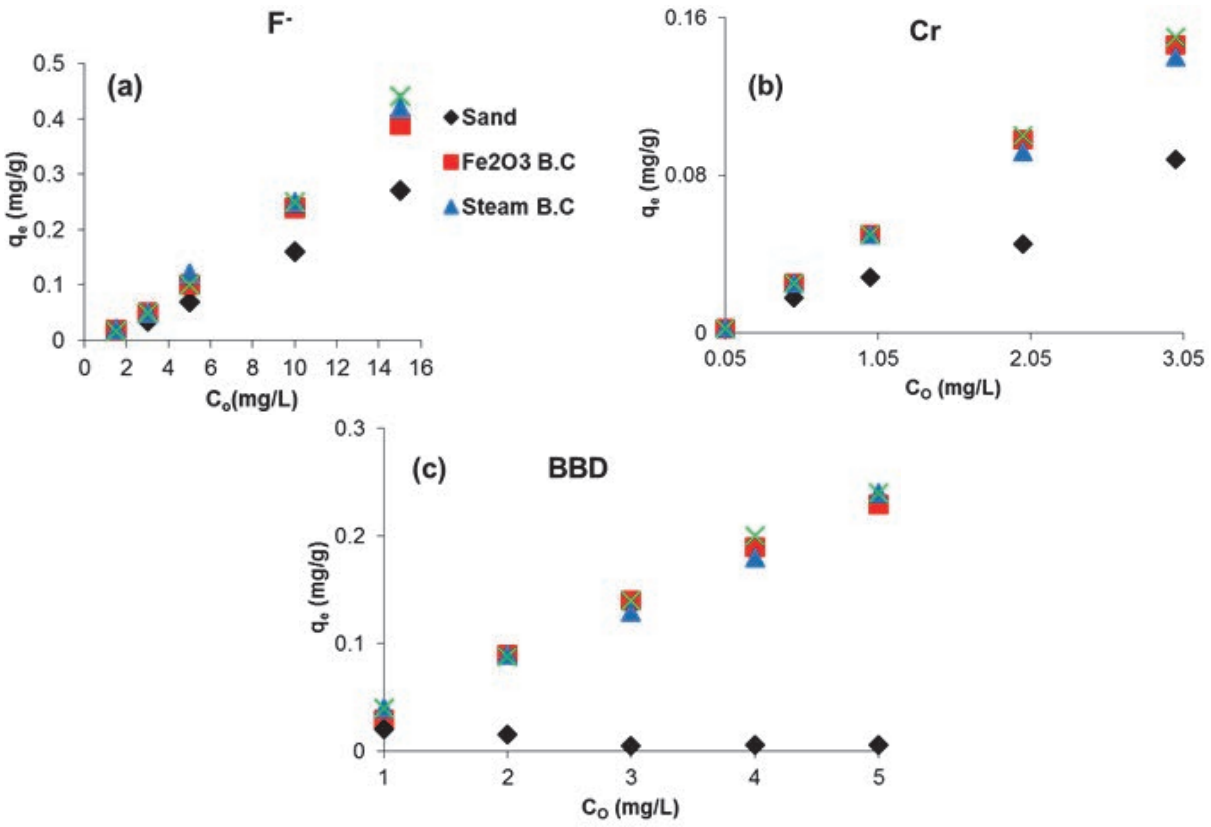

Fig. 6. Influence of initial concentration of (a) F^-, (b) Cr, and (c) BBD on the adsorbent's adsorption capacities at solution pH of 5.1, 2 g/100 mL adsorbent dosage, and 120 min contact time at room temperature (23-25 °C). Error bars show standard errors of the mean (n=3)

However, despite being quenched from the top, BC had a higher removal capacity than SBC, which was quenched from the bottom, perhaps due to other mechanisms involved in the pollutant removal process. Due to limited porosity, adsorption on sand occurs mainly at liquid-solid interface due to van der Waals forces, trapping contaminants on its surface. Biochar based adsorbents adsorb the contaminants both via van der Waals interactions and chemical bonding within their internal and external surfaces (Tran et al., 2017).

Batch experiments results showed that BC is the best adsorbent with adsorption capacity of 0.44, 0.15, and 0.24 mg/g for F^-, Cr, and BBD, respectively; and there were no significant differences between Fe_2O_3-BC, SBC, and BC at p = 0.971, 0.314, and 0.993 for F^-, Cr, and BBD, respectively. For BBD removal, there was a significant difference between biochar based adsorbents and the control (sand) (p = 0). The batch adsorption experiment results did not agree with the hypothesis that Fe_2O_3-BC has high adsorption capacity than SBC and BC. This might be because the red clay soil used to prepare iron water for producing magnetic biochar was not effective in removing F^- from water.

3.2.4. Adsorption isotherms

Fitting pollutant adsorption data onto BC to isotherm models showed that F^- adsorption was well described by the Freundlich model (r^2=0.939), while BBD (r^2=0.822) and Cr (r^2=0.845) were adequately described by the Langmuir model (Fig. 7). The F^- and BBD batch adsorption data followed the Freundlich model, indicating that adsorption occurred on multilayer heterogeneous sites (Belhachemi and Addoun, 2011), whereas the adsorption of Cr was on the finite monolayer adsorption sites within the adsorbents (Pelosi et al., 2014). These results are consistent with similar batch studies reported in literature (e.g., Arora and Tiwari, 2017; Dong et al., 2011; Man and Mandal, 2014; Zhou et al., 2014a).

3.2.5. Thermodynamics of adsorption

Batch adsorption experiments were performed at 298 K, and the data used to estimate ΔG^0 (Eq. 12) (Chaukura et al., 2017):

$$\Delta G^0 = -RTLnK \quad (12)$$

where K is a constant from the best fitting model, R (8.314 J/mol.K) is the universal gas constant, T (K) is the temperature.

The calculated ΔG^0 values for adsorption onto BC were -4.79, -2.72, and -1.82 kJ/mol for F^-, Cr, and BBD, respectively. The values *of* ΔG^0<0, indicating adsorption is feasible and spontaneous (Tong et al., 2019). Previous studies on the adsorption of BBD onto Fe_3O_4-BC and BC at 298 K reported ΔG^0 values of -5.932 and -7.344 kJ/mol, respectively (Chaukura et al., 2017; Tong et al., 2019).

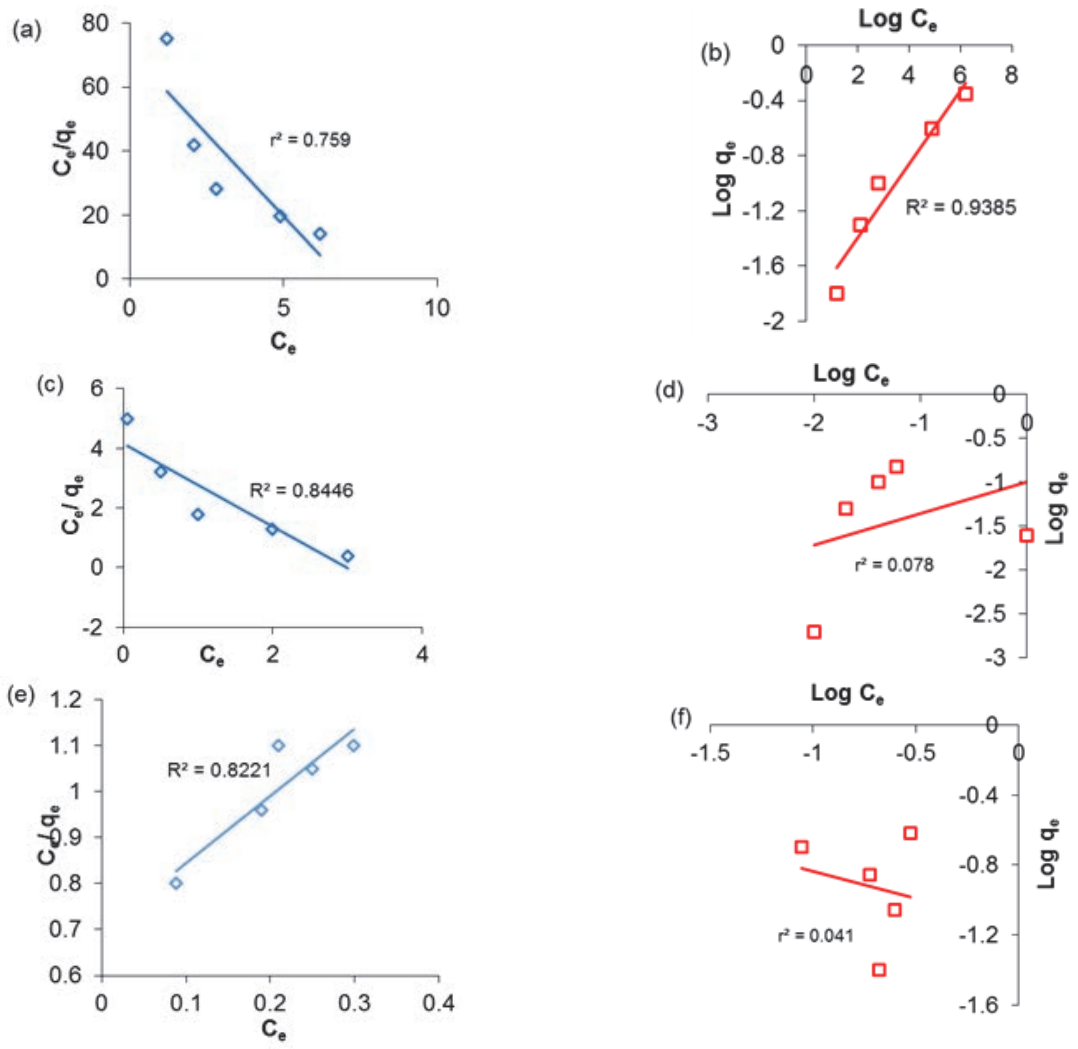

Fig. 7. (a) F^- Langmuir, (b) F^- Freundlich, (c) Cr Langmuir, (d) Cr Freundlich, (e) BBD Langmuir, and (f) BBD Freundlich isotherms for the adsorption of pollutants onto BC

Enthalpy change (ΔH^0) and entropy change (ΔS^0) can be determined from experiments that measure adsorption at varying temperatures. Overall, thermodynamic parameters such as ΔH^0, ΔS^0, and ΔG^0 are important for practical process applications such as prototype design.

3.3. Column Experiments

3.3.1. Fluoride Removal

The layered biochar column reached breakthrough point at 1.83 mg/L after treating 133 mL, and exhaustion point at 10.4 mg/L having treated 797.4 mL (Fig. 8a). The sand and biochar mixed column reached breakthrough point at 1.5 mg/L after treating 129.9 mL, and exhaustion point at 9.9 mg/L after treating 779.4 mL. In the sand column, breakthrough point was reached 1.96 mg/L after treating a volume of 150 mL, and exhaustion was attained at 14.8 mg/L having treated 425 mL. The mass of adsorbent required to treat the fluoride at breakthrough point was 526, 557 and 806.2 g/L for the layered column, sand and biochar mixture column, and the sand column, respectively. There was a significant difference between the layered biochar column, sand and biochar mixed column and the sand column ($p = 0$). However, there was no significant difference between layered biochar column, and sand and biochar mixed column ($p = 0.885$).

3.3.2. Chromium removal

The layered biochar column reached breakthrough point at 0.25 mg/L after treating 310 mL and exhaustion point at 0.62 mg/L having treated 797.4 mL (Fig. 8b). The sand and biochar mixed column reached breakthrough point at 0.22 mg/L after treating 303 mL, and exhaustion point at 0.59 mg/L after treating 779.4 mL.

In the sand column, breakthrough point was reached at 0.64 mg/L after treating effluent volume of 25 mL, and the exhaustion mark was at 14.8 mg/L having treated 450 mL. The mass of adsorbent required to treat the F^- at breakthrough point was 225.48, 238.8 g, and 4837.2 g/L for the layered column, sand and biochar mixed column, and sand column, respectively.

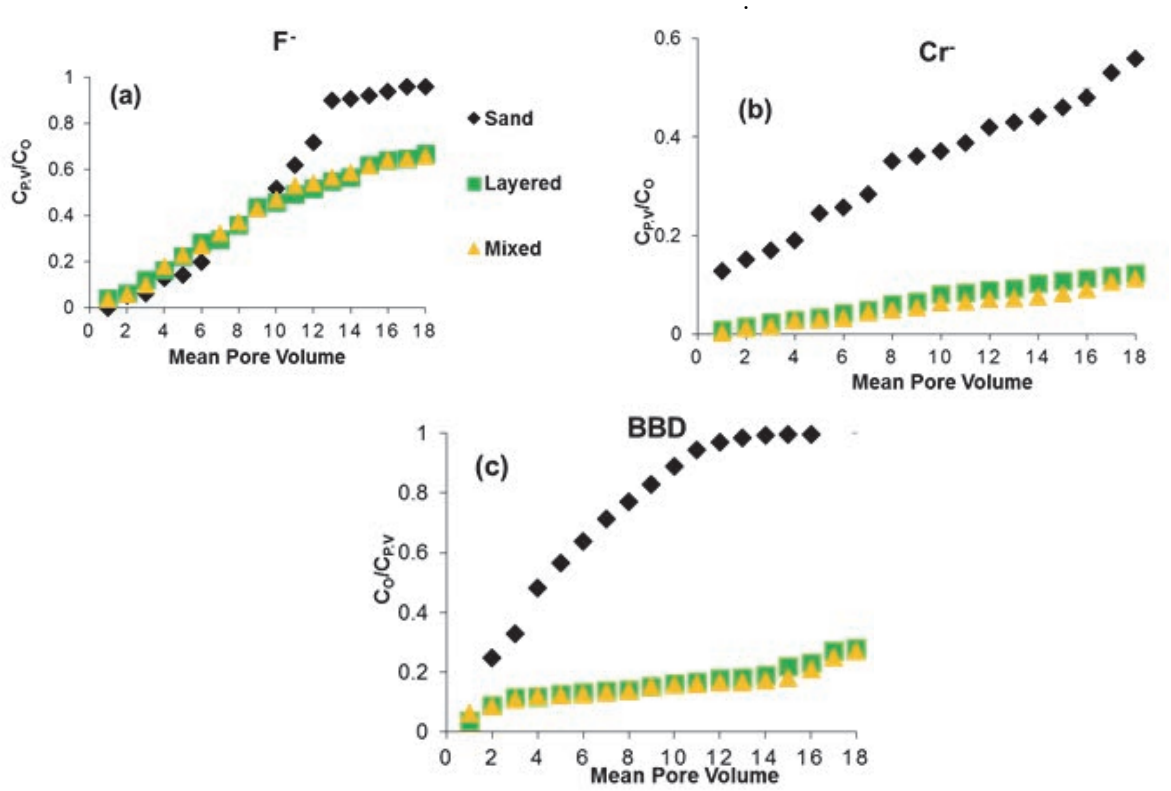

Fig. 8. Breakthrough curves for layered biochar, sand and biochar mixture, and sand column at (a) initial F concentration of 15 mg/L, (b) initial Cr concentration of 5 mg/L, and (c) initial BBD concentration of 5 mg/L. The pH was 5, bed depth 10 cm, and temperature 23-25 ^oC. Error bars showed the standard errors of the mean (n=3)

Whereas there is significant difference between the layered biochar column, sand and biochar mixed column and the sand column (p = 0), there was no significant difference between layered biochar column and sand and biochar mixed column (p = 0.055).

3.3.3. Brilliant blue dye removal

The sand and biochar mixed column reached breakthrough point at 0.43 mg/L after treating 130 mL and exhaustion mark at 1.44 mg/L having treated 779.4 mL (Fig. 8c). The layered column reached breakthrough point at 0.47 mg/L after treating 132.9 mL, and exhaustion point at 1.33 mg/L having treated 797.4 mL. The sand column reached breakthrough mark at 0.21 mg/L after treating 150 mL, and an exhaustion mark at 4.93 mg/L after treating 450 mL. The r^2 values were 0.912, 0.822, and 0.46 for the layered column, sand and biochar mixed column, and the sand column, respectively. The respective masses of adsorbent required to treat brilliant blue dye at breakthrough point were 525.96, 557.3, and 806.2 g/L. There was a significant difference between layered biochar column, sand and biochar mixed column and the control sand (p = 0).

The experimental data fitted the Thomas and Logit models well for F^- adsorption with the r^2 values of 0.91, 0.885, and 0.565 for layered, sand and biochar mixed, and sand columns, respectively (Fig 9). Adsorption evaluation through the Logit model showed that for layered biochar, the adsorption rate constant (K) was 0.0138 L/mg.h, while for the sand and biochar mixture column K = 0.0128 L/mg. h, and for the sand column K = 0.01 L/mg.h

For Cr adsorption, the Logit model showed that K values were 0.017, 0.015, and 0.0635 L/mg.h for the layered column, sand and biochar mixed column, and the sand column, respectively. The results showed that there was no significant differences between layered column, sand and biochar mixed column on the adsorption of Cr, F^- and BBD. There are however, significant differences between layered column and mixed column compared to sand (control) (p = 0); data from the layered column was well described by the Logit and Thomas models with r^2 = 0.99, 0.959, and 0.912 for F^-, Cr, and BBD, respectively. The layered column had the lowest adsorbent mass requirement of 526, 225.48, and 525.96 g/L for F^-, Cr, and BBD, respectively.

The absence of significant differences between layered column and sand and biochar mixed column for F^-, Cr and BBD removal is influenced by use of similar adsorbent material (BC). This adsorbent determines the adsorption mechanism and trend, hence the layered and mixed columns followed the same trend at difference magnitude as shown by different r^2 values. The existence of significant difference between layered and mixed columns compared to sand is influenced by differences in adsorbent particle arrangement, packing density, and porosity of the materials. Layered column data fitted

the Thomas and Logit models closely compared to the mixed column (Fig. 9), implying that in layered column adsorption mechanism occurred through interphase mass transfer (Zhang et al., 2015). The arrangement of sand and biochar in the mixed columns allowed for interphase mass transfer as the adsorbate solution comes in contact with the fixed adsorbent in the filter bed. This results in continuous exchange of physical and chemical adsorption phases due to presence of sand layer prior to biochar, followed by sand and biochar layers in the filter bed compared to mixed columns where both occur in one mixed filter bed (Ndé-tchoupé et al., 2015).

The layered arrangement of the filter bed results in less adsorbent material being required at breakthrough for F^-, Cr and BBD removal compared to the mixed column arrangement. The layered arrangement allows interphase mass transfer during adsorption resulting in attaining high exhaustion volume and high adsorption zone bed height, higher discharge, flow velocity and less residence time as compared to mixed as the adsorbate solution is treated in layers. Overall, the layered configuration was the best filter bed arrangement, requiring less mass (526 g/L) of adsorbent, while the sand column was the worst, requiring 806.2 g/L. These results are comparable to other fixed bed adsorption studies previously reported in literature (e.g., Ali 2014; Dong et al., 2011; Kumar and Acharya, 2012; Okewale et al., 2015; Zhang et al., 2015). The column experiment results confirmed the hypothesis that the layered biochar column had higher adsorption capacity than sand and biochar mixture column. However, the results show that biochar based adsorbents have higher removal capacity than sand columns.

Overall, this work showed that pristine biochar synthesised from Brachystegia spiciformis hardwood commonly used as firewood for household cooking and heating can be used for water treatment.

The design parameters experimentally determined from breakthrough curve of column experiments are: height of adsorption zone was found to be 9.28 cm and the rate at which the adsorption zone was moving through the bed was 0.3 cm/h. The percentage of the total column saturated at breakthrough was found 47.96 %. Discharge through the column was 2.16 $\times 10^{-2}$ L/h and the flow velocity was 7.018 cm/h. The value of adsorption rate coefficient (K) 0.0138 L/ (mg.h) and adsorption capacity coefficient (N) was 129.236 mg/L. Mass of biochar used was 69.9 g in the 10 cm column. Volume of effluent treated at breakthrough point was 0.133 L and the mass of adsorbed required is 525.56 g/L.

A comparison of the adsorbents studied herein with those in literature show that while F- removal was lower, it was of the same order of magnitude with previous studies (Table 2). Cr and BBD removal was comparable to methods using adsorption, but lower than biomass treated with sodium bicarbonate.

5. Conclusions and outlook

This study investigated a water treatment system for the removal of F^-, Cr and BBD in ternary aqueous systems using biochar adsorbents synthesized through 'KonTiki' flame curtain pyrolysis. Characterization results based on SEM-EDS showed that F^-, Cr and BBD were adsorbed on the biochar adsorbent pore spaces and outer surfaces.

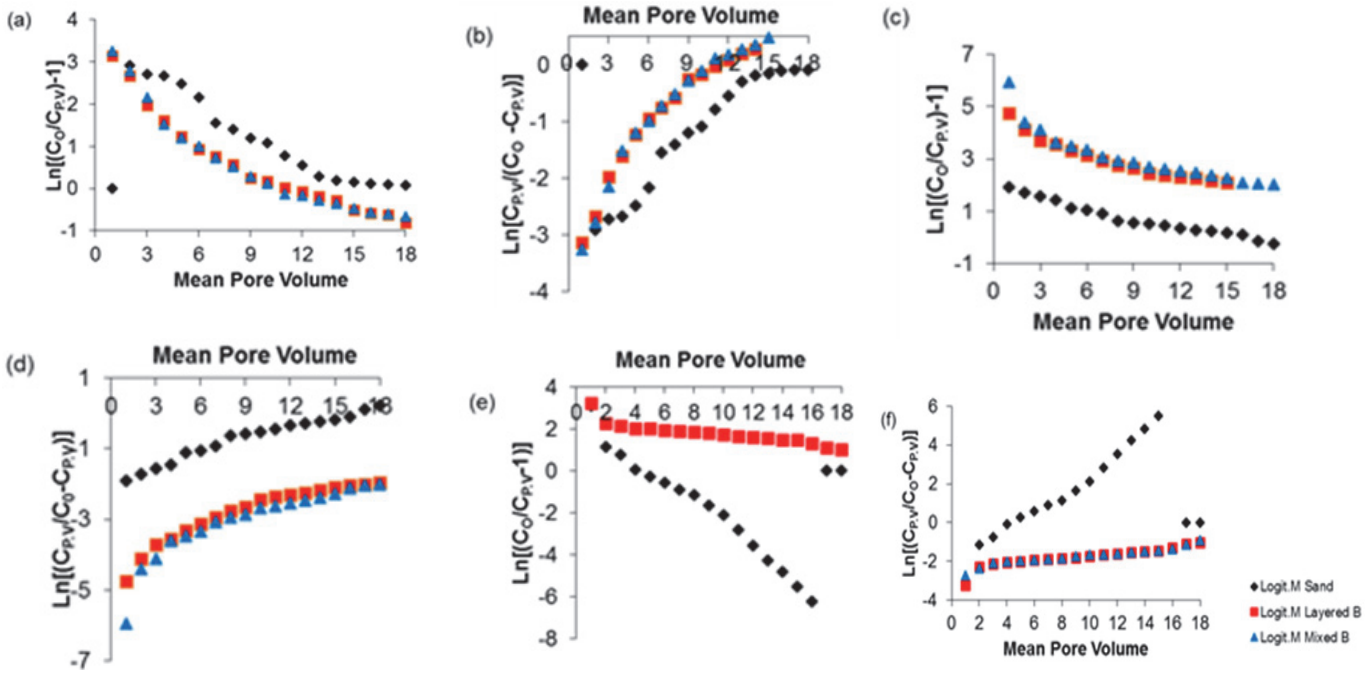

Fig. 9. (a) F^- Thomas, (b) F^- Logit, (c) Cr Thomas, (d) Cr Logit, (e) BBD Thomas, and (f) BBD Logit isotherms for the adsorption of pollutants onto BC

Table 2. A comparison of the performance of the materials with those reported in literature

Removal method/material	*Removal capacity*	*Remarks*	*Reference*
Sodium bicarbonate treated carbon	Brilliant blue dye 237.2 mg/g	Batch adsorption experiments; solution pH of 7.0 and an adsorbent dose of 0.4 g/L	Periyaraman et al., 2019
Membrane capacitive deionization	F^-: 2.7554 mg/g, Cr(IV): 3.227 mg/g	Membrane capacitive deionization for 100 mg/L solution, using an electrode fabricated from wood apple shell activated carbon	Gaikwad and Balomajumder, 2018
Physically activated *Ceiba pentandra* seeds	Methylene blue dye 324.01 mg/g	Batch experiments; contact time: 60 min; pH:7.0; temperature: 30 ^{0}C	Manikandan et al., 2018
Chemically activated *Ceiba pentandra* seeds	Methylene blue dye 469.4 mg/g	Batch experiments; contact time: 60 min; pH: 7.0; temperature: 30 ^{0}C	Manikandan et al., 2018
Pseudomonas stutzeri and acid treated Banyan tree bark	Cr(IV) 27.47 mg/g	A mixture of acid treated Banyan tree bark and *Pseudomonas stutzeri* was used as an adsorbent.	Yaashikaa et al., 2019
A hybrid Fe-Al anode	F^-: 41.1 mg/L; Cr(IV): 49.99 mg/L	A combined electrocoagulation-electroflotation for simultaneous removal of F^- and Cr(IV)	Aoudj et al., 2015
BC	F^-: 9.7; Cr(IV): 24.0 mg/g; BBD: 14.3 mg/g		Present work

Preliminary adsorbents evaluation in batch experiments showed that pristine biochar was the best adsorbent, and it was subsequently used throughout the research alongside the control sand adsorbent. F^- adsorption was best described by the Freundlich model, while the Langmuir model best described Cr and BBD adsorption.

The layered biochar was the best column configuration with highest r^2 value of 0.91 using non-linear regression Thomas and Logit model fitting. The layered filter required lowest adsorbent mass of 526 g/L for F^-, Cr and BBD removal. The optimum column design used for the fixed bed adsorption experiments is 3 cm in diameter, packed to a bed depth of 10 cm and a column height of 24.2 cm.

Future work should measure the surface charge on the adsorbents, and investigate the regeneration of exhausted adsorbents for multiple reuse. This is important in assessing the economic feasibility of the field application of the POU device.

In conclusion, a pristine biochar synthesised from *Brachystegia spiciformis* hardwood commonly used as firewood fuel for cooking and heating is a useful adsorbent for the removal of F^-, Cr and BBD in water. This can potentially be useful in designing point-of-use water purification systems for poor communities.

Acknowledgements

The authors are grateful for the financial support received from the International Foundation for Science (IFS), Sweden (grant number C/5266-2) awarded to Prof. Willis Gwenzi.

References

Ali I., (2014), Water treatment by adsorption columns: evaluation at ground level water treatment by adsorption columns: Evaluation at ground level, *Separation and Purification Reviews*, **43**, 175-205.

Arora V., Tiwari D.P., (2017), Adsorption of brilliant blue dye using activated walnut shell powder, *International Journal of Advanced Technology in Engineering and Science*, **5**, 248-255.

Belhachemi A., Addoun F., (2011), Comparative adsorption isotherms and modeling of methylene blue onto activated carbons, *Journal of Applied Water Science*, **1**, 111-117.

Chaukura N., Murimba E.C., Gwenzi W., (2017), Synthesis, characterisation and methyl orange adsorption capacity of ferric oxide – biochar nano-composites derived from pulp and paper sludge, *Applied Water Science*, **7**, 2175-2186.

Chen N., Zhang Z., Feng C., Li M., Chen R., Sugiura N., (2011), Investigations on the batch and fixed-bed column performance of fluoride adsorption by Kanuma mud, *Desalination*, **268**, 76-82.

De Gisi S., Lofrano G., Grassi M., Notarnicola M., (2016), Characteristics and adsorption capacities of low-cost sorbents for wastewater treatment: A review, *Sustainable Materials and Technologies*, **9**, 10-40.

Dong X., Ma L.Q., Li Y., (2011), Characteristics and mechanisms of hexavalent chromium removal by biochar from sugar beet tailing, *Journal of Hazardous Materials*, **190**, 909-915.

Duku M.H., Gu S., Hagan E.B., (2011), Biochar production potential in Ghana - A review, *Renewable Sustainable Energy Review*, **15**, 3539-3551.

Dutta M., Ray T., Basu J.K., (2012), Batch adsorption of fluoride ions onto microwave assisted activated carbon derived from *Acacia Auriculiformis* scrap wood, *Archives of Applied Science Research*, **4**, 536-550.

Gaikwad M.S., Balomajumder C., (2018), Removal of Cr(VI) and fluoride by membrane capacitive deionization with nanoporous and microporous Limonia acidissima (wood apple) shell activated carbon electrode, *Separation and Purification Technology*, **195**, 305-313.

Grassi M., Kaykioglu G., Belgiorno V., Lofrano G., (2012), *Removal of Emerging Contaminants from Water and Wastewater by Adsorption Process*, In: *Emerging Compounds Removal from Wastewater*, Lofrano G. (Eds.), SpringerBriefs in Molecular Science, Springer, Dordrecht, 15-37.

Gupta V.K., Carrott P.J.M., Carrott M.M.L.R., (2009), Low-cost adsorbents : growing approach to wastewater treatment - a review. *Critical Review in Environmental Science and Technology*, **39**, 783-842.

Gwenzi W., Chaukura N., Mukome F., Machado N.D., Nyamasoka B., (2015), Biochar production and applications in sub-Saharan Africa: Opportunities, constraints, risks and uncertainties, *Journal of Environmental Management*, **150**, 250-261.

Gwenzi W., Chaukura N., Noubactep C., Mukome F.N.D., (2017), Biochar-based water treatment as a potential low-cost and sustainable technology for clean water provision, *Journal of Environmental Management*, **197**, 732-749.

Gwenzi W., Musarurwa T., Nyamugafata P., Chaukura N., Chaparadza A., Mbera S., (2014), Adsorption of Zn^{2+} and Ni^{2+} in a binary aqueous solution by biosorbents derived from sawdust and water hyacinth (*Eichhorniacrassipes*), *Water Science and Technology*, **70**, 1419-1427.

Kong X., Liu Y., Pi J., Li W., Liao Q., (2017), Low-cost magnetic herbal biochar: characterization and application for antibiotic removal, *Environmental Science and Pollution Research*, **24**, 6679-6687.

Kumar U., Acharya J., (2012), Fixed bed column study for the removal of copper from aquatic environment by NCRH, *Global Journal of Researchers in Engineering*, **12**, 0-4.

Mamuse A., Watkins R., (2016), High fluoride drinking water in Gokwe, North West Zimbabwe, *Journal of Water, Sanitation, & Hygiene for Development*, **6**, 55-64.

Manikandan G., Kumarb P.S., Saravanan A., (2018), Modelling and analysis on the removal of methylene blue dye from aqueous solution using physically/chemically modified *Ceiba pentandra* seeds, *Journal of Industrial and Engineering Chemistry*, **62**, 446-461.

Mishra V., Sureshkumar M., Gupta N., Kaushik P., (2017), Study on sorption characteristics of uranium onto biochar derived from Eucalyptus Wood, *Water, Air, & Soil Pollution*, **228**, 1-14.

Mohan D., Sarswat A., Sik Y., Pittman Jr. C.U., (2014), Organic and inorganic contaminants removal from water with biochar, a renewable, low cost and sustainable adsorbent - A critical review, *Bioresource Technology*, **160**, 191-202.

Mohan D., Sharma R., Singh V.K., Steele P., Pittman Jr. C.U., (2012), Fluoride removal from water using biochar, a green waste, low-cost adsorbent: equilibrium uptake and sorption dynamics modeling, *Industrial and Engineering Chemistry Research*, **51**, 900-914.

Mon J., Flury M., Harsh J.B., (2006), Sorption of four triarylmethane dyes in a sandy soil determined by batch and column experiments, *Geoderma*, **133**, 217-224.

Ndé-tchoupé A.I., Crane R.A., Mwakabona H.T., Noubactep C., Njau K.N., (2015), Technologies for decentralized fluoride removal: testing metallic iron-based filters, *Journal of Water MDPI*, **7**, 6750-6774.

Oh S., Seo Y., Kim B., Kim I.Y., Cha D.K., (2016), Microbial reduction of nitrate in the presence of zero-valent iron and biochar, *Bioresource Technology*, **200**, 891-896.

Okewale A.O., Igbokwe P.K., Babayemi K.A., (2015), Design of pilot packed column for the dehydration of water from ethanol-water mixtures, *Advances in Chemical Engineering and Science*, **5**, 152-157.

Periyaraman P.M., Karan S., Ponnusamy S.K., Vaidyanathan V., Vasanthakumar S., Dhanasekaran A., Subramanian S., (2019), Adsorption of an anionic dye onto native and chemically modified agricultural waste, *Environmental Engineering and Management Journal*, **18**, 257-270.

Schmidt H., Taylor P., (2014), Kon-Tiki flame curtain pyrolysis for the democratization of biochar production, *Ithaka-Journal for Biochar Materials, Ecosystems and Agriculture*, Arbaz, Switzerland, ISSN 1663-0521, pp. 338 -348, www.ithaka-journal.net/86.

Shang J., Pi J., Zong M., Wang Y., Li W., Liao Q., (2016), Chromium removal using magnetic biochar derived from herb-residue, *Journal of the Taiwan Institute of Chemical Engineers*, **68**, 289-294.

Sujitha R., Ravindhranath K., (2016), Removal of Coomassie brilliant blue dye from waste waters using active carbon derived from barks of *Ficus racemosa* plant, *Der Pharmacia Lettre*, **8**, 72-83.

Tobayiwa C., Musiyambiri M., Chironga L., Mazorodze O., Sapahla S., (1991), Fluoride levels and dental fluorosis in two districts in Zimbabwe, *Central African Journal of Medicine*, **37**, 353-361.

Togarepi E., Mahamadi C., Mangombe A., (2012), Defluoridation of water using physico-chemically treated sand as a low-cost adsorbent: An equilibrium study, *African Journal of Environmental Science and Technology*, **6**, 176-181.

Tong Y., McNamara P.J., Mayer B.K., (2019), Adsorption of organic micropollutants onto biochar: a review of relevant kinetics, mechanisms and equilibrium, *Environmental Science.: Water Research & Technology*, **5**, 821-838.

Tran H., You N., Bandegharaei S., Chao H.P., (2017), Mistakes and inconsistencies regarding adsorption of contaminants from aqueous solutions: A critical review, *Water Research*, **120**, 88-116.

UN, (2015), *17 Sustainable Development Goals*, Edited by UNDP, Geneva, On line at: sustainabledevelopment.un.org/partnership/unsummit2015.

Vermeulen S.J., Campbell B.M., Matzke G.E., (1996), The consumption of wood by rural households in Gokwe communal area, Zimbabwe, *Human Ecology*, **24**, 479-491.

Wang S., Gao B., Li Y., Creamer A.E., He F., (2017), Adsorptive removal of arsenate from aqueous solutions by biochar supported zero-valent iron nano composite: Batch and continuous flow tests, *Journal of Hazardous Materials*, **322**, 172-181.

WHO, (2011), *Guidelines for Drinking-water Quality*, 4th Edition, World Health Organisation, Geneva, On line at: http://www.who.int.

Xue S., Jin W., Zhang Z., Liu H., (2017), Reductions of dissolved organic matter and disinfection by-product precursors in full-scale wastewater treatment plants in winter, *Chemosphere*, **179**, 395-404.

Yaashikaa P.R., Kumar P.S., Babu V.P.M., Durga R.K., Manivasagan V., Saranya K., Saravanan A., (2019), Modelling on the removal of Cr(VI) ions fromaquatic systemusing mixed biosorbent (*Pseudomonas stutzeri* and acid treated Banyan tree bark), *Journal of Molecular Liquids*, **276**, 362-370.

Zhang M., Ahmad M., Al-wabel M. I., Vithanage M., Rajapaksha A.U., Kim H.S., Lee S.S., Ok Y.S., (2015), Adsorptive removal of trichloroethylene in water by crop residue biochars pyrolyzed at contrasting

temperatures: continuous fixed-bed experiments, *Journal of Chemistry*, **2015**, 1-6, http://dx.doi.org/10.1155/2015/647072.

Zhou H., Chen W., Zhang X., Shi D., (2014), Preparation of nanometer magnesia and its properties for fluoride removal, *Frontiers of Environmental Science*, **3**, 97-108.

Zhou Y., Gao B., Zimmerman A.R., Chen H., Zhang M., Cao X., (2014), Biochar-supported zero valent iron for removal of various contaminants from aqueous solutions, *Bioresource Technology*, **152**, 538-542.